



Bimetallic Rh–Ni/BN catalyst for methane reforming with CO₂

Jeffrey C.S. Wu*, Hui-Chen Chou

Department of Chemical Engineering, National Taiwan University, No. 1, Section 4, Roosevelt Road, Taipei 10617, Taiwan, ROC

ARTICLE INFO

Article history:

Received 2 November 2008

Received in revised form 7 January 2009

Accepted 8 January 2009

Keywords:

Dry reforming

Methane

Carbon dioxide

Syngas

Boron nitride

Ni

Rh

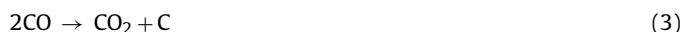
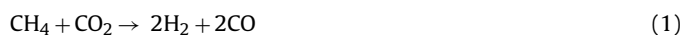
ABSTRACT

The dry reforming of methane (CH₄) with carbon dioxide (CO₂) was carried out using bimetal (Rh–Ni)-loaded boron nitride (BN) and γ -Al₂O₃ catalysts. The incipient wetness method was used to load different ratios of Rh/Ni on BN and γ -Al₂O₃ supports. The metal particles were too small to be observed in the XRD indicating highly dispersed Rh–Ni particles on the supports. XPS results showed that, after H₂ reduction at 500 °C, Rh became metallic element while most Ni remained in its oxidized state. The addition of Rh increased the activity of dry reforming as well as the stability of the catalysts. In general, the conversions of CH₄ with CO₂ on Rh–Ni/BN catalysts were higher than those on Rh–Ni/ γ -Al₂O₃ catalysts. The optimum ratio of Rh/Ni loading on BN was 0.01. The ratio of H₂ and CO as the products was near 0.7. The maximum conversions of CH₄ and CO₂ reached 72% and 81%, respectively, at 700 °C, while only slight deactivation was observed after 6 h of reaction time. Boron nitride has many unique properties, such as inertness and negligible metal-support interference, as compared with traditional oxide supports. Metal particles can migrate freely and easily to form Rh–Ni clusters on the BN surface. This may be the origin of the activity enhancement in dry reforming.

© 2009 Elsevier B.V. All rights reserved.

1. Introduction

Carbon dioxide is one of the major greenhouse gases that lead to global warming. Hydrogen is one of the best alternative energies. The reforming of CH₄ with CO₂ (also called dry reforming) provides an effective way to solve both problems, that is, CO₂ remediation and H₂ production. In this process, valuable syngas, H₂ and CO, can be obtained based on Eq. (1). Since this reaction is strongly endothermic, high temperature is quite favorable for the reaction. Despite this fact, high temperature may also have detrimental effect on the catalyst as well as the reaction because coke formation may occur during CH₄ cracking (Eq. (2)) and CO disproportionation (Eq. (3)) [1]. Furthermore, H₂ can also be consumed by CO₂ to form water and generate excess CO as shown in Eq. (4). Metal sintering is considered to be one of the major causes of catalyst deactivation in dry reforming because the reaction is usually carried out above 700 °C.



Inui et al. performed CH₄ reforming with CO₂ to generate H₂ on Ni based catalysts at 700 °C and indicated that the precious metals, Rh and Pt, may enhance the reaction rate markedly. This synergistic effect is ascribed to H₂ spillover on the surface of the precious metals [2]. Loading of transition metals, such as Ru and Pd, also strongly improves the activity and stability of Ni based catalysts for CH₄ reforming with CO₂ [3]. The improved activity is attributed to the formation of Ni–Ru cluster with increasing Ni dispersion that causes the formation of reactive intermediate carbonaceous species. One difficulty of dry reforming is to achieve high CH₄ conversion and H₂ selectivity simultaneously. Traditionally, Ni catalyst is used in CH₄ reforming with CO₂ at temperature of above 700 °C [4]. Coke formation can be significantly reduced by Rh addition, which increases the stability of the catalysts. Jozwiak et al. reported that SiO₂ supported monometallic Ni, Rh and bimetallic Ni–Rh catalysts are comparably good catalysts for CH₄ reforming with CO₂ and Rh-rich catalysts are resistant to deactivation and carbon formation, resulting in high CH₄ conversion and H₂ selectivity [5–7].

Materials traditionally used as supports are insulating oxides such as SiO₂, γ -Al₂O₃, V₂O₅, TiO₂ and various zeolites. These oxides possess large surface area, numerous acidic/basic sites, and metal-support interaction that offer particular catalytic activity for many reactions. Metal oxides have also been thoroughly studied and employed in the chemical industry for decades. On the other hand, non-oxide materials, unlike metal oxides, possess many unique properties, such as high thermal conductivity, acid–base resistance, hydrophobicity and possibly negligible metal-support interaction. Boron nitride has been used as catalyst support recently [8,9]. The

* Corresponding author. Tel.: +886 223631994; fax: +886 223623040.
E-mail address: cswu@ntu.edu.tw (J.C.S. Wu).

graphite-like hexagonal BN is the most stable BN isomer under ambient conditions [10]. In general, BN is inert for catalytic reaction. In a supported metal system such as Pt/BN, BN has been shown to have negligible interaction with Pt in the catalytic oxidation [8]. The migration of Pt particles occurred easily on the crystalline face of BN due to the weaker adhesion between the crystalline face and Pt [8,9]. Such effect may lead to the formation of bimetallic clusters. Our previous study indicated that Pt–Sn alloy on BN support significantly enhanced the oxidative dehydrogenation of propane with less coking [11]. The migration of a particular metal species to the surface will affect catalytic properties, such as adsorption, oxidation and reduction. The bimetallic clusters are favorable for dry reforming to reduce coking. Therefore, for the first time, CH₄ reforming with CO₂ is selected to explore the enhanced activity and selectivity toward H₂ generation by the bimetallic clusters on the unique BN support.

2. Experimental

2.1. Catalysts preparation

Hexagonal-BN was obtained from the High Performance Materials Inc. (Taiwan). It was crystallized at roughly 800 °C during synthesis, a temperature lower than the typical 1000 °C. Gamma alumina (γ -Al₂O₃), a commonly used oxide support, was obtained from Merck (USA) and used for comparison. Precursor salt, Ni(NO₃)₂·6H₂O, with 20.18 wt% nickel (Ni) and pure RhCl₃ with 48.7 wt% rhodium (Rh) were purchased from Alfa Aesar (USA). Methanol was chosen as the diluting solvent for improved soaking of the hydrophobic BN support. The supported Rh–Ni catalysts were prepared by the co-incipient wetness method. The quantity of methanol required to completely fill the support's pore volume was predetermined. Calculated amounts of Rh and Ni precursor salts were dissolved in methanol to obtain the desired metal loading. After the co-incipient wetness process, catalysts were air-dried at room temperature for 48 h. These are referred to as fresh catalysts. The Rh loading was varied from 0.1 to 1 wt% and the Ni loading was varied from 1.0 to 10.0 wt%. The nomenclature of catalyst with X wt% Rh and Y wt% Ni on BN support was assigned as RhXNiY/BN. In addition, 1 wt% Rh/BN, 10 wt% Ni/BN and the counterparts in Rh–Ni/ γ -Al₂O₃ were also prepared for comparison. The detailed incipient wetness procedure is described in literature [12].

2.2. Characterization

The specific surface area of the support was determined from N₂ adsorption measured by Micromeritics ASAP 2010. The particle sizes and distributions of BN and γ -Al₂O₃ were measured by laser-light scattering. γ -Al₂O₃ was suspended and dispersed ultrasonically in water for 3 min. BN was dispersed in ethanol due to its hydrophobicity. Coulter LS 230 was used to measure the scattering of incident light at the 90° position, thereafter the particle size was calculated using the Fraunhofer equation. Hydrogen chemisorption was measured by Micromeritics Autochem II. Fresh catalyst was reduced in 10% H₂/Ar flow at 500 °C for 1 h then cooled down to 50 °C under He purge before H₂ pulse chemisorption. Each pulse contained 0.05 ml of 10% H₂/Ar and the time between pulses was 3 min. The value of H₂ chemisorption was taken to determine Rh+Ni dispersion by assuming H:metal = 1.

A transmission electron microscope (TEM, Hitachi H-7100) was employed to observe the shape of BN and the appearance of metal particles dispersed on the support. The crystalline phases of catalysts were identified by X-ray diffraction (XRD). The XRD equipment, type M03XHF22 from the Material Analysis and Characterization Company, was operated at 40 kV, with a X-ray of

1.54056 Å in wavelength from a Cu target, and a scanning speed of 0.5°/min. X-ray photoelectron spectroscopy (XPS) was conducted on a spectrometer of VG Microtech MT500. The measured binding energy was referenced to carbon (1 s) at 285.6 eV.

2.3. Methane reforming with CO₂

Fresh catalyst (0.06 g) was charged in the middle of a straight-tube quartz reactor with a 10-mm ID. The catalyst was reduced for 1 h at 500 °C using pure hydrogen (99.999%) in the reactor. Subsequently, the temperature was increased to the reaction temperature under Ar purge before switching to the reactant mixture. In some cases, the fresh catalyst was calcined in air at 300 °C followed by the H₂ reduction as mentioned above. The reactant mixture was composed of pure CH₄ and CO₂. The CH₄/CO₂ mixture, with molar ratio maintained at one, was passed through the reactor at a total flow rate of 55 ml/min (WHSV = 60 l/(g-cat h)) under atmospheric pressure. The concentration of CH₄ and CO₂ in the reactant mixture was accurately adjusted by tuning the corresponding flow meter. The concentration was further confirmed by an on-line GC (Agilent GC6890) before reaction. The reaction temperatures were maintained at 600, 700 and 800 °C in a tubular furnace. A thermocouple was placed in the center of the catalyst bed to record the reaction temperature and to control the furnace. The reformato was analyzed by the on-line GC equipped with a 30 m Supelco Carboxen 1006 Plot capillary column using FID and TCD detectors in series.

The conversions of CH₄ and CO₂ as well as the yields of H₂ and CO were calculated using Eqs. (5)–(8) [13]. In order to estimate the amount of coke formed, the overall carbon balance was calculated based on the difference of input and output total hydrocarbons.

$$\text{CH}_4 \text{ conversion (\%)} = \frac{\text{moles of CH}_4 \text{ converted}}{\text{moles of CH}_4 \text{ in feed}} \times 100 \quad (5)$$

$$\text{CO}_2 \text{ conversion (\%)} = \frac{\text{moles of CO}_2 \text{ converted}}{\text{moles of CO}_2 \text{ in feed}} \times 100 \quad (6)$$

$$\text{CO yield (\%)} = \frac{\text{moles of CO produced}}{\text{moles of CH}_4 \text{ in feed} + \text{moles of CO}_2 \text{ in feed}} \times 100 \quad (7)$$

$$\text{H}_2 \text{ yield (\%)} = \frac{\text{moles of H}_2 \text{ produced}}{2 \text{ moles of CH}_4 \text{ in feed}} \times 100 \quad (8)$$

3. Results

3.1. Characteristics of catalysts

The specific surface areas of BN and γ -Al₂O₃ are 47.2 and 112.2 m²/g, respectively. The mean particle size of BN and γ -Al₂O₃ were calculated to be 3.7 and 77.4 μ m, respectively, from the measurement of laser-light scattering. Table 1 summarizes the results of H₂ chemisorption and metal dispersion of all catalysts. Since the chemisorption of Rh and Ni cannot be distinguished, all surface metals (M_{sur}), including Rh and Ni, are counted together. The metal dispersion, M_{sur}/M_{bulk}, is estimated from H_{ad}/M_{bulk} ratio assuming chemisorption stoichiometry H/M = 1 for both monometallic and bimetallic catalysts [5]. In general, the amount of H₂ chemisorbed on γ -Al₂O₃ catalyst is higher than that on BN catalyst, implying higher metal dispersion on γ -Al₂O₃ due to the nature of support. For the monometallic catalyst, the metal dispersion of Rh is much higher than that of Ni on γ -Al₂O₃ and BN supports. As compared with Ni catalyst, the amount of H₂ chemisorbed on Rh–Ni catalyst increased upon Rh addition. This suggests that the chemisorption of H₂ on Rh–Ni catalyst is attributed mostly to Rh because of the incomplete reduction of Ni by H₂ at 500 °C (see XPS in Fig. 5). Leclercq et al. reported that Ni could not be completely reduced at

Table 1
H₂ chemisorption and metal dispersion and particle size.

Catalyst	Hydrogen atom (ml/g)	Metal dispersion (%)
Ni10/BN	0.382	0.9
Rh0.1Ni10/BN	0.808	1.9
Rh0.1Ni1/BN	0.044	1.0
Rh1Ni1/BN	0.106	1.6
Rh1/BN	0.092	3.9
Ni10/ γ -Al ₂ O ₃	1.194	2.9
Rh0.1Ni10/ γ -Al ₂ O ₃	1.582	3.8
Rh0.1Ni1/ γ -Al ₂ O ₃	0.524	11.9
Rh1Ni1/ γ -Al ₂ O ₃	0.216	3.3
Rh1/ γ -Al ₂ O ₃	0.556	23.4

Reduced at 500 °C in H₂ before chemisorption, metal dispersion = hydrogen atom/loaded (Ni atom + Rh atom).

450 °C on Ni–Rh bimetallic catalysts and Ni hardly adsorbed hydrogen. In addition, they found the Ni surface enrichment on the Ni–Rh catalysts [14]. That is, Ni–Rh clusters could partially cover by Ni, which suppressed the H₂ chemisorption resulting in low metal dispersion in Table 1. In general, the dispersion of Rh and Ni metals on BN is lower than that on γ -Al₂O₃ because metals are easily migrated and sintered to form large metal particles on slippery BN surface during H₂ reduction.

Fig. 1 shows the XRD patterns of BN, Rh1/BN, Ni10/BN and series of RhNi/BN catalysts which were H₂ reduced at 500 °C. The diffraction pattern of Rh1/BN is similar to that of pure BN. The highest diffraction peak of Rh is at 41.1° which overlapped with that of BN. The diffraction peak of Rh at 47.8° can be barely observed on Rh1/BN. The major diffraction peaks of Ni at 44.5° and 51.8° can only be identified for high Ni loading catalysts, Ni10/BN and Rh0.1Ni10/BN. No diffraction peaks of Rh and Ni can be found in Rh1Ni1/BN and Rh0.1Ni1/BN implying that metal particles are very small. Fig. 2 shows the XRD patterns of γ -Al₂O₃, Rh1/ γ -Al₂O₃, Ni10/ γ -Al₂O₃ and series of Rh–Ni/ γ -Al₂O₃ catalysts, which were H₂ reduced at 500 °C. They appear to be the same as the background diffraction pattern of γ -Al₂O₃ alone. Even the high Ni loading catalysts, Ni10/ γ -Al₂O₃ and Rh0.1Ni10/ γ -Al₂O₃, do not display the major Ni diffraction peaks located at 44.5° and 51.8°. The metal particles are too small to be observed from the XRD patterns, revealing highly dispersed Ni and Rh–Ni metal particles on the γ -Al₂O₃ support. Based on the results of H₂ chemisorption and XRD, these catalysts exhibit a wide distribution in metal particle size.

Fig. 3 shows the TEM images of Ni10/BN and Rh0.1Ni10/BN. Most metal particles with sizes <10 nm can be observed in Fig. 3(a), which indicates that most of the Ni particles are located on the edges

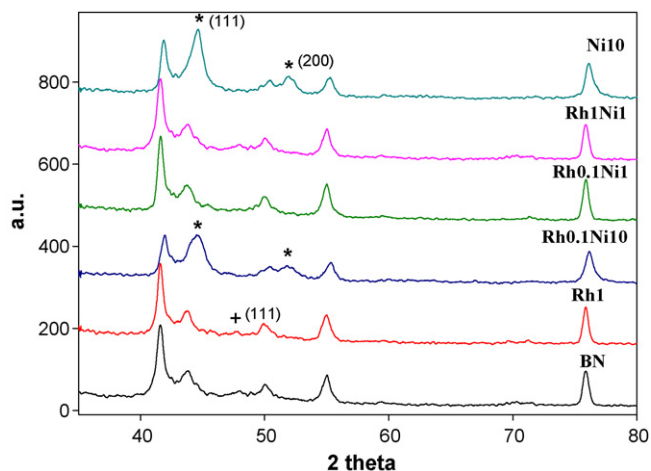


Fig. 1. XRD of BN, Rh1/BN, Ni10/BN and series of RhNi/BN, H₂ reduced at 500 °C for 1 h Ni(*) and Rh(+).

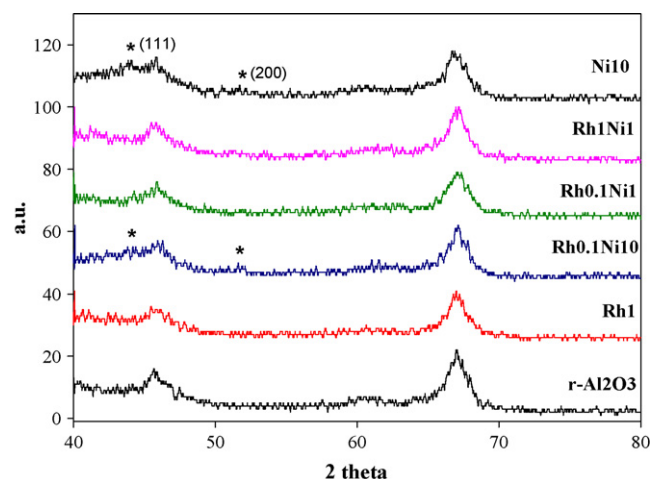


Fig. 2. XRD of γ -Al₂O₃, Rh/ γ -Al₂O₃, Ni/ γ -Al₂O₃ and RhNi/ γ -Al₂O₃, H₂ reduced at 500 °C for 1 h Ni(*).

of BN particles. The metal particles <10 nm are also observed on Rh0.1Ni10/BN as shown in Fig. 3(b). However, Rh, Ni or Rh–Ni cluster cannot be distinguished from each other on the BN support.

The chemical status of Rh and Ni on the fresh and H₂ reduced Rh1Ni1/BN catalysts were investigated by XPS and shown in Figs. 4 and 5, respectively. As shown in Fig. 4, the binding energy of Rh 3d_{5/2} in H₂ reduced Rh1Ni1/BN is detected at 308.6 eV indicating metal Rh⁰, whereas that in fresh Rh1Ni1/BN is located near 310.2 eV suggesting Rh³⁺ state as in the precursor RhCl₃ [15]. As shown in Fig. 5, the binding energy of Ni 3p_{1/2} in fresh Rh1Ni1/BN is at 873.0 eV indicating Ni²⁺ state as in the precursor Ni(NO₃)₂. After H₂ reduction at 500 °C, the binding energy of Ni 3p_{1/2} on Rh1Ni1/BN is slightly shifted to 872.5 eV indicating most of Ni remains as Ni²⁺ state on BN support [15]. Similar results are also found in the XPS of Rh–Ni/ γ -Al₂O₃ (not shown). Thus after H₂ reduction at 500 °C, the surface Rh is mostly reduced but large portion of Ni²⁺ still remains oxidized. Based on the semi-quantitative XPS analysis, the molar ratio of Ni/Rh after H₂ reduction is twice as much as that before H₂ reduction, suggesting Rh⁰ could be partially covered by Ni²⁺ on Rh–Ni/BN catalyst.

3.2. Methane reforming with CO₂

Various pretreatment procedures were investigated based on CH₄ conversions and H₂ yields of the catalysts performed in the temperature range between 600 and 800 °C. Catalysts were either calcined in air at 300, 400 and 500 °C, or reduced with hydrogen at temperature ranging from 300 to 500 °C. In summary of experimental results, the conversion of CH₄ and CO₂ increased from 20% to 80% and 25% to 92%, respectively, as the temperature was varied from 600 to 800 °C, while H₂ yield changed from less than 5% up to 65% depending on the reaction conditions. Although CH₄ conversion of higher than 80% can be reached at 800 °C, CO₂ conversion was decreased due to coke formation according to Eq. (3). Meanwhile, H₂ yield was significantly reduced to 35% because hydrogen is oxidized by CO₂ to produce water (Eq. (4)). In conclusion, the optimal temperature of calcination and H₂ reduction is found to be at 300 and 500 °C, respectively. The highest H₂ yield is found to be at reaction temperature of 700 °C, which gives a H₂/CO ratio of near 0.7. Accordingly, a reaction temperature of 700 °C was selected for the detailed study of the catalysts.

Table 2 summarizes the overall performances, including CH₄ conversion, H₂ and CO yields, of catalysts initially (0 h) and at 6-h period under reaction temperature of 700 °C. The stability of catalysts is defined as the percentage change of 6-h and initial

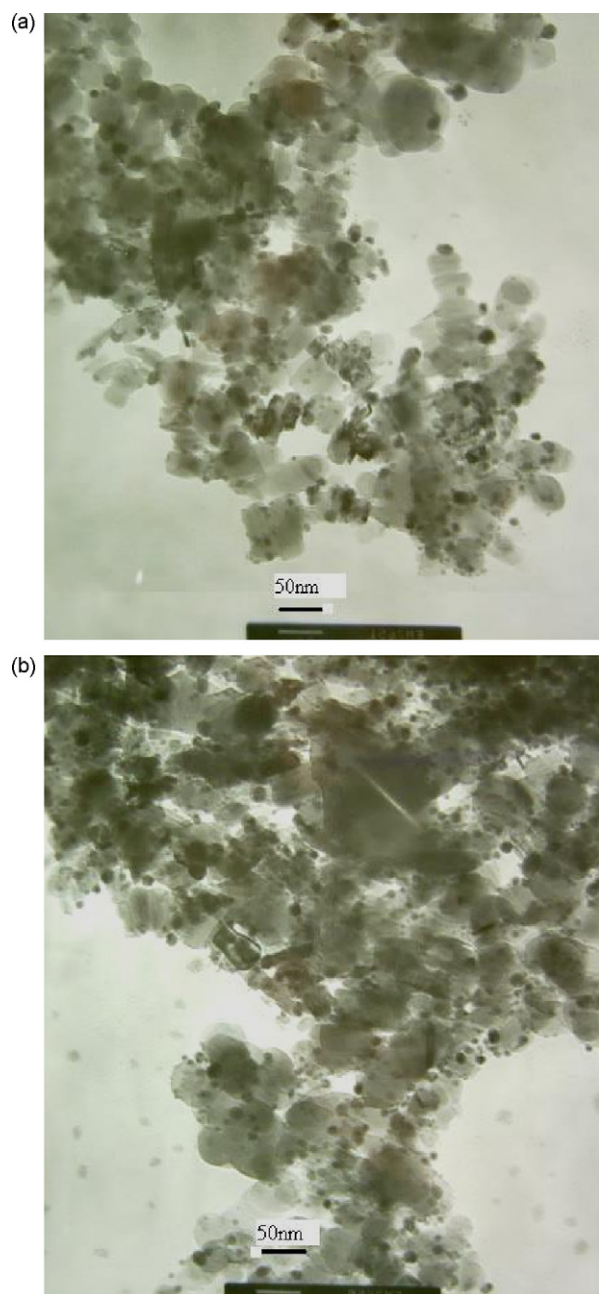


Fig. 3. TEM of (a) Ni10/BN and (b) Rh0.1Ni10/BN.

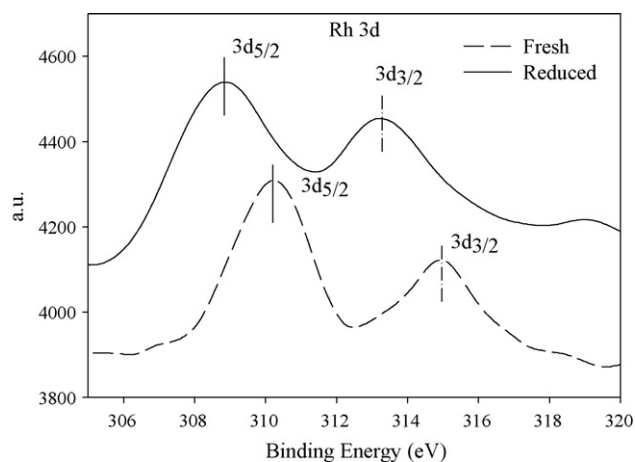


Fig. 4. XPS of Rh 3d on Rh1Ni1/BN.

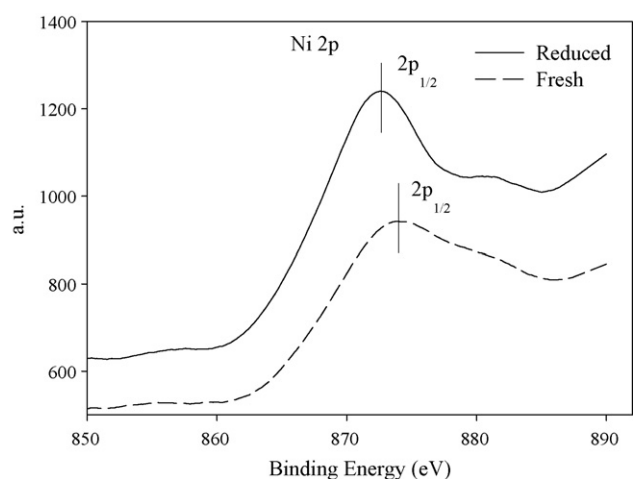


Fig. 5. XPS of Ni 2p on Rh1Ni1/BN.

methane conversions [6]. The number of stability implies the activity variation of catalysts in dry reforming. These catalysts were H₂ reduced at 500 °C prior to reaction. It is noted that Rh/BN and Rh/ γ -Al₂O₃ give the lowest CH₄ conversion as expected because Rh is not a reforming catalyst. The CH₄ conversion of Ni10/BN and Ni10/ γ -Al₂O₃ are almost the same (~50%) initially. However, deactivation of Ni10/BN is more significant than that of Ni10/ γ -Al₂O₃. The CH₄ conversion is either increased or decreased with Rh addition on bimetallic Rh–Ni catalysts. For Rh–Ni/ γ -Al₂O₃, a negative effect on CH₄ conversion is found. The CH₄ conversion decreases with

Table 2

Summary of CH₄ reforming with CO₂ on Rh–Ni catalysts at 700 °C.

Catalyst ^a (%)	CH ₄ conversion (%)		CO ₂ conversion (%)		H ₂ yield (%)		CO yield (%)		Stability ^b (%)
	0 h	6 h	0 h	6 h	0 h	6 h	0 h	6 h	
Rh1/BN	27.6	9.5	32.0	9.2	17.9	4.2	31.6	5.3	–65.6
Rh1Ni1/BN	42.1	42.4	65.3	50.9	38.9	26.9	76.7	51.4	0.7
Rh0.1Ni1/BN	36.9	32.0	61.2	49.2	53.9	32.1	74.3	57.9	–13.3
Rh0.1Ni10/BN	70.4	49.6	81.0	62.4	60.2	55.5	78.4	71.0	–29.5
Ni10/BN	50.6	29.7	60.7	44.1	40.3	12.2	52.2	37.0	–41.3
Rh1/ γ -Al ₂ O ₃	2.5	0.9	7.6	0.5	8.7	0.6	16.0	1.1	–64.0
Rh1Ni1/ γ -Al ₂ O ₃	45.0	36.1	60.3	48.2	38.9	31.8	72.0	58.8	–19.8
Rh0.1Ni1/ γ -Al ₂ O ₃	27.6	2.3	39.6	4.2	53.2	8.6	51.7	9.4	–91.7
Rh0.1Ni10/ γ -Al ₂ O ₃	47.9	44.1	66.0	61.1	42.3	36.1	76.3	68.7	–7.9
Ni10/ γ -Al ₂ O ₃	51.8	47.0	70.0	62.0	42.3	30.5	76.9	65.8	–9.3

^a Catalysts were H₂ reduced at 500 °C for 1 h before reaction.

^b Defined as (6-h conv. of CH₄ – initial conv. of CH₄)/initial conv. of CH₄ × 100%.

Table 3
Summary of CH₄ reforming with CO₂ on calcined Rh–Ni catalysts at 700 °C.

Catalyst ^a (%)	CH ₄ conversion (%)		CO ₂ conversion (%)		H ₂ yield (%)		CO yield (%)		Stability ^b (%)
	0 h	6 h	0 h	6 h	0 h	6 h	0 h	6 h	
Rh1/BN	11.5	2.2	22.8	6.6	27.8	5.8	37.2	9.9	–80.9
Rh1Ni1/BN	42.8	38.3	63.6	59.0	64.0	40.4	78.0	71.6	–10.5
Rh0.1Ni1/BN	65.0	42.2	68.2	51.9	59.4	48.2	68.8	52.6	–35.1
Rh0.1Ni10/BN	72.4	68.9	88.3	86.0	62.2	61.1	88.1	81.4	–4.8
Ni10/BN	55.9	29.7	56.4	28.5	42.4	40.7	55.0	31.8	–46.9
Rh1/γ–Al ₂ O ₃	0.1	0.6	0.9	1.4	1.0	0.0	3.8	0.7	500.0
Rh1Ni1/γ–Al ₂ O ₃	44.4	33.0	58.3	42.7	38.6	26.1	69.5	51.2	–25.7
Rh0.1Ni1/γ–Al ₂ O ₃	21.5	4.2	26.6	7.6	13.8	2.4	18.5	2.8	–80.5
Rh0.1Ni10/γ–Al ₂ O ₃	53.6	55.2	74.0	78.0	66.0	51.1	76.0	85.4	3.0
Ni10/γ–Al ₂ O ₃	46.5	42.9	61.8	57.4	57.7	29.2	76.3	70.1	–7.7

^a Catalysts were calcined at 300 °C for 2 h followed by H₂ reduction at 500 °C for 1 h.

^b Defined as (6-h conv. of CH₄ – initial conv. of CH₄)/initial conv. of CH₄ × 100%.

various Rh/Ni ratios. However, it is substantially increased to 70.4% on Rh0.1Ni10/BN while other Rh–Ni/BN catalysts show less CH₄ conversion than that of Ni10/BN. Furthermore, H₂ and CO yields of Rh0.1Ni10/BN are also the highest among all catalysts. As compared with monometallic Ni/BN catalyst, both CH₄ conversion and H₂ yield of Rh0.1Ni10/BN are significantly improved concurrently.

Table 3 summarizes the overall performances of catalysts performed under the same condition as described earlier in Table 2 with the exception of the pretreatment procedure. A calcination step was applied to the catalysts in air at 300 °C prior to H₂ reduction at 500 °C. It appears that the initial CH₄ conversions of bimetallic Rh–Ni catalysts in Table 3 are higher than those in Table 2, except Rh0.1Ni1/γ–Al₂O₃. Similarly, H₂ yields in Table 3 are also higher than those in Table 2, with the exception of Rh0.1Ni1/γ–Al₂O₃. The performance of Rh-containing monometallic catalyst is the worst among other monometallic catalysts shown in Tables 2 and 3. The performances of Ni10/BN and Ni10/γ–Al₂O₃ are worse than those of Rh–Ni/BN and Rh–Ni/γ–Al₂O₃, respectively. To sum up the results listed in Tables 2 and 3, the calcination pretreatment procedure of fresh catalyst at 300 °C followed by H₂ reduction at 500 °C can improve both the activity and stability of bimetallic Rh–Ni catalysts.

The stability of a catalyst is the percentage change of CH₄ conversions during dry reforming in 6 h. As shown in Tables 2 and 3, bimetallic catalysts are more stable than monometallic Ni catalysts on BN support. The major cause of deactivation in catalyst is due to coke formation. The degree of coking can be deduced from the rate of carbon deposition, which is estimated by the carbon balance. Table 4 lists the carbon balances of all catalysts during 6-h reforming. A negative carbon balance means that carbon is deposited on the catalyst. The coking is more severe initially because CH₄ is decomposed rapidly by some highly active sites on the fresh catalyst (Eq. (2)). Less coking is found on Rh–Ni catalysts as compared with Ni catalysts. After 6 h of reaction, the coke formation on Rh–Ni/BN catalysts is slightly less than that on Rh–Ni/γ–Al₂O₃ catalysts.

Table 4
Carbon balances for CH₄ reforming with CO₂ on various catalysts at 700 °C.

Catalyst	Initial (0 h) (%) ^a	Final (6 h) (%) ^a
Rh1/BN	–5.32	–3.57
Rh1Ni1/BN	–9.83	–4.53
Rh0.1Ni1/BN	–9.32	–5.44
Rh0.1Ni10/BN	–13.74	–5.87
Ni10/BN	–15.50	–7.03
Rh1/γ–Al ₂ O ₃	–2.44	–3.14
Rh1Ni1/γ–Al ₂ O ₃	–8.13	–5.45
Rh0.1Ni1/γ–Al ₂ O ₃	–13.31	–5.74
Rh0.1Ni10/γ–Al ₂ O ₃	–14.01	–8.33
Ni10/γ–Al ₂ O ₃	–16.11	–9.12

^a (moles of carbon output – moles of carbon input)/(moles of carbon input) × 100%.

Fig. 6 shows the dependency of CH₄ conversion on reaction time for Rh1, Ni10 and Rh–Ni/BN catalysts performed at 700 °C. The pretreatment of the catalysts is the same as that described for Table 3. It is obvious that the conversions are gradually decreased during the 6-h reaction period. Among the catalysts

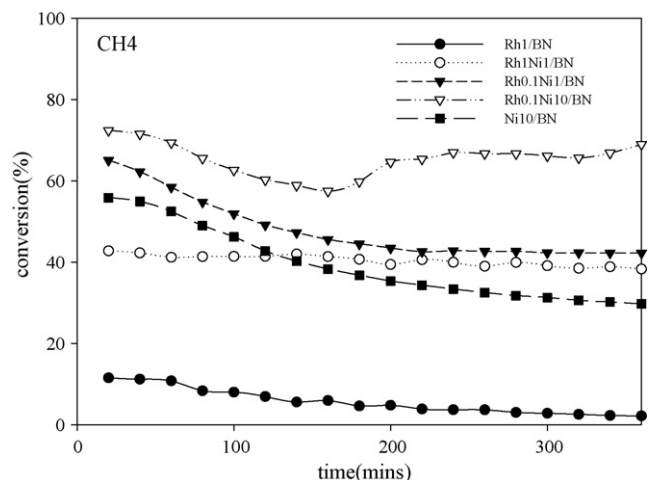


Fig. 6. CH₄ conversions of dry reforming on Ni and Ni–Rh catalysts at 700 °C. (Catalysts were calcined in air at 300 °C, then H₂ reduced at 500 °C, weight = 0.06 g, pressure = 1 atm, total flow rate = 55 ml/min, CH₄/CO₂ = 1/1.)

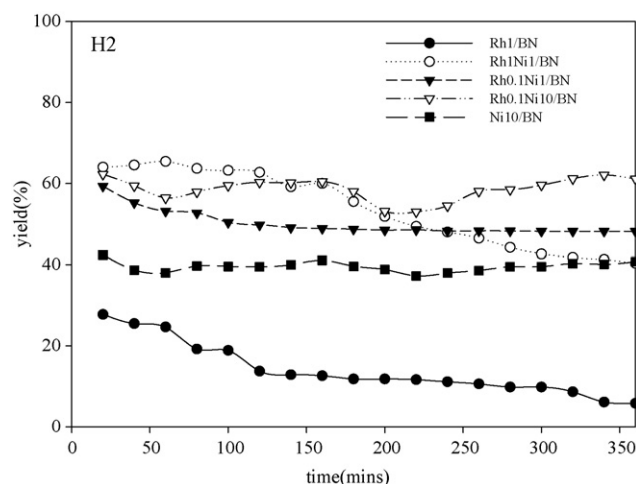


Fig. 7. H₂ yields of dry reforming on Ni and Ni–Rh catalysts at 700 °C. (Catalysts were calcined in air at 300 °C, then H₂ reduced at 500 °C, weight = 0.06 g, pressure = 1 atm, total flow rate = 55 ml/min, CH₄/CO₂ = 1/1.)

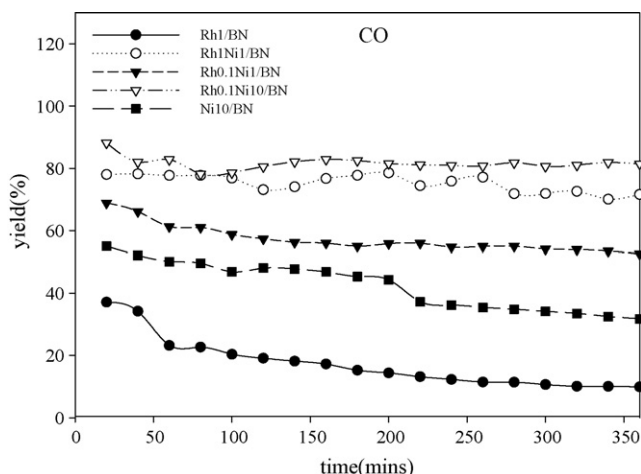


Fig. 8. CO yields of dry reforming on Ni and Ni-Rh catalysts at 700 °C. (Catalysts were calcined in air at 300 °C, then H₂ reduced at 500 °C, weight = 0.06 g, pressure = 1 atm, total flow rate = 55 ml/min, CH₄/CO₂ = 1/1.)

tested, Rh0.1Ni10/BN gives the highest CH₄ conversion and H₂ yield, which is also higher than its counterpart, Rh0.1Ni1/γ-Al₂O₃ (not shown). The plots of H₂ and CO yields versus time for catalysts (Rh1/BN, Ni10/BN and Rh–Ni/BN) performed at 700 °C are shown in Figs. 7 and 8, respectively. Clearly, the H₂ and CO yields of monometallic Rh1/BN and Ni10/BN catalysts are lower than those of bimetallic Rh–Ni/BN catalysts. Compared with various Rh and Ni loadings on Rh–Ni/BN catalysts, Rh0.1Ni10/BN gives the highest H₂ and CO yields. The H₂ and CO yields reach 62% and 88% initially, followed by a slight decrease to 61% and 81%, respectively, with some fluctuations.

The effects of catalyst regeneration on the catalytic performance in terms of CH₄ conversion for Rh0.1Ni10/BN and Rh0.1Ni10/γ-Al₂O₃ are illustrated in Fig. 9. In the regeneration process, the catalysts were calcined again at 300 °C to remove carbon deposit after the first 6-h run. Despite the fact that the conversions of CH₄ in the second run have declined for both catalysts, the activity of Rh0.1Ni10/BN still outperformed that of Rh0.1Ni10/γ-Al₂O₃. Moreover, the degree of deactivation for Rh0.1Ni10/BN is less than that for Rh0.1Ni10/γ-Al₂O₃, indicating that the regeneration process under air is more effective for BN support.

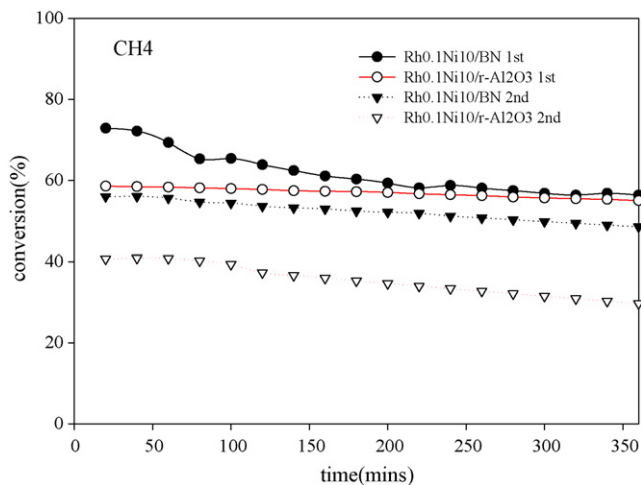


Fig. 9. CH₄ conversions of dry reforming in the regeneration test on Rh0.1Ni10/BN and Rh0.1Ni10/γ-Al₂O₃ at 700 °C. (Catalysts were calcined in air at 300 °C, then H₂ reduced at 500 °C; after first run, catalysts were calcined again in air at 300 °C for 2 h in the reactor, weight = 0.06 g, pressure = 1 atm, total flow rate = 55 ml/min, CH₄/CO₂ = 1/1.)

4. Discussion

Rhodium plays a major role in the reduction of coke and the enhancement of H₂ yield. Hydrogen spillover on Rh is believed to suppress coke formation from CO (Eq. (3)) as well as the hydrogenation of CO₂ (Eq. (4)) [2]. The synergistic effect of bimetallic catalyst can increase CH₄ conversion as well as H₂ yield in dry reforming, which is evidenced by the performance of both Rh–Ni/BN and Rh–Ni/γ-Al₂O₃ catalysts. The stability of bimetallic Rh–Ni catalyst was improved due to less coke formation as compared with that of monometallic Ni catalyst [5].

Besides the Rh effect, support can also be an important factor affecting the activity in CH₄ dry reforming. By and large, the stabilities of Rh–Ni/BN catalysts are close to those of Rh–Ni/γ-Al₂O₃ catalysts as shown in Tables 2 and 3. However, CH₄ conversions and H₂ yields are substantially enhanced on Rh–Ni/BN catalysts as compared with Rh–Ni/γ-Al₂O₃ catalysts, even though the metal dispersion on BN is less than that on γ-Al₂O₃ (Table 1). Boron nitride provides an inert and slippery surface that facilitates the formation of Rh–Ni cluster during H₂ reduction at 500 °C due to the unrestrained migration of metals. On the other hand, γ-Al₂O₃ usually constrains the mobility of Rh and Ni during H₂ reduction owing to the metal-support affinity, thus separating Rh and Ni particles. For this reason, Rh–Ni clusters are much easily formed on BN surface. The Rh–Ni cluster on BN surface is composed of Rh⁰ particle partially covered with Ni²⁺ (Table 1, Figs. 4 and 5). Therefore, Ni²⁺ on BN may become more active in CH₄ activation than that on γ-Al₂O₃, which is suggested to be the origin of the activity enhancement in CH₄ dry reforming. In addition, the neutral BN surface is favorable to CH₄ dry reforming. Our previous study indicated that acidic site on BN is much less than that on γ-Al₂O₃ [9]. Coke formation is less severe on the BN surface resulting in higher activity as compared with γ-Al₂O₃ for long-term reaction.

5. Conclusion

This study has presented favorable findings for the dry reforming of CH₄ with CO₂ into H₂ and CO by employing BN-supported Rh–Ni catalysts. Compared with the traditional γ-Al₂O₃ support, BN exhibits a unique property of minimum metal-support interference thus facilitates the formation of Rh–Ni clusters during H₂ reduction. The yield of H₂ is improved without sacrificing the conversion of CH₄. Coke formation is slightly reduced on BN due to the lack of acidic sites. Therefore, BN offers a promising support for dry reforming catalyst.

Acknowledgment

The authors would like to thank the National Science Council of the Republic of China, Taiwan for financially supporting this research under Contract No. NSC-94-2214-E-002-029.

References

- [1] J.R. Rostrupnielsen, J.H.B. Hansen, *J. Catal.* 144 (1993) 38–49.
- [2] T. Inui, K. Saigo, Y. Fujii, K. Fujioka, *Catal. Today* 26 (1995) 295–302.
- [3] C. Crisafulli, S. Scire, R. Maggiore, S. Mimico, S. Galvagno, *Catal. Lett.* 59 (1999) 21–26.
- [4] X.E. Verykios, *Int. J. Hydrogen Energy* 28 (2003) 1045–1063.
- [5] W.K. Jozwiak, M. Nowosielska, J. Rynkowski, *Appl. Catal. A: Gen.* 280 (2005) 233–244.
- [6] Z. Hou, P. Chen, H. Fang, X. Zheng, T. Yashima, *Int. J. Hydrogen Energy* 31 (2006) 555–561.
- [7] Z.Y. Hou, T. Yashima, *Catal. Lett.* 89 (2003) 193–197.
- [8] C.-A. Lin, J.C.S. Wu, J.-W. Pan, C.-T. Yeh, *J. Catal.* 210 (2002) 39–45.
- [9] J.C.S. Wu, Y.C. Fan, C.A. Lin, *Ind. Eng. Chem. Res.* 42 (2003) 3225–3229.
- [10] S. Alkoy, C. Toy, T. Gonul, A. Tekin, *J. Eur. Ceram. Soc.* 17 (1997) 1415–1422.

- [11] J.C.S. Wu, S.-J. Lin, *Chem. Eng. J.* 140 (2008) 391–397.
- [12] J.C.S. Wu, Z.-A. Lin, J.-W. Pan, M.-H. Rei, *Appl. Catal. A: Gen.* 219 (2001) 117–124.
- [13] N. Sahli, C. Petit, A.C. Roger, A. Kiennemann, S. Libs, M.M. Bettahar, *Catal. Today* 113 (2006) 187–193.
- [14] G. Leclercq, S. Pietrzyk, L. Gengembre, L. Leclercq, *Appl. Catal.* 27 (1986) 299–312.
- [15] J.F. Moulder, J. Chastain, R.C. King, *Handbook of X-ray Photoelectron Spectroscopy: A Reference Book of Standard Spectra for Identification and Interpretation of XPS Data*, Physical Electronics, Eden Prairie, MN, 1995.